Single-molecule Study on the Interactions between Cyclic Nonribosomal Peptides and Protein Nanopore

Shuo Zhou^{1,#}, Han Wang^{1,2,#}, Xiaohan Chen³, Yunjiao Wang^{1,2}, Daming Zhou¹, Liyuan Liang^{1,2}, Liang Wang^{1,2,*}, Deqiang Wang^{1,2,*} and Xiyun Guan^{3,*}

- ¹ Chongqing Institute of Green and Intelligent Technology, Chinese Academy of Sciences, Chongqing 400714, China
- ² University of Chinese Academy of Sciences, Beijing 100049, China
- ³ Department of Chemistry, Illinois Institute of Technology, Chicago, IL 60616, USA
- [#] These authors contributed equally to this work.

Supporting Information

ABSTRACT: Nonribosomal peptides (NRPs) are a type of secondary metabolites mostly originated from microorganisms such as bacteria and fungi. Their proteolytic stability, highly selective bioactivity, and microorganism-specificity have made them an attractive source of drugs for the pharmaceutical industry. Herein, with microcystins (MCs) as a NRP model, we, for the first time, proposed a sensitive method to study the interactions between NRPs and the protein nanopore. Due to the large molecular size (\sim 3 nm diameter) of MCs and their net negative charges, MCs failed to translocate through the α -hemolysin (α -HL) protein channel. Our results demonstrated that the biomolecular interaction of MC- α -HL protein was significantly affected by the applied potential bias. The constant blockage amplitude in the voltage-dependent studies indicated that the current modulation events were dominantly contributed to the bumping interaction between MCs and the α -HL protein under the electrophoretic force. The mean residence time of the bumping events exhibited a two-stage decrease (from 1.90 ms to 1.02 ms, and from 1.02 ms to 0.69 ms) at the threshold voltages of -70 mV and -100 mV, respectively. Using our strategy (i.e., based on their electrophoretic driven interaction with the α -HL protein pore), discrimination of different MC molecules (MC-LR, MC-RR, MC-YR and linear analog) with varied branched residues could be accomplished. This work should provide an insight in developing a rapid and effective method for the identification of cyclic NRPs as valuable biomarkers for fungal infections.

Key Words: Nanopore, Nonribosomal Peptides, Microcystins, Molecular Transport, Biomarker

1. Introduction

Biological nanopores, inspired from transmembrane ion channels, are proteins and peptides which can regulate the passage of cargos such as ions and other charged or polar molecules. The regulation is in principle controllable via the selective states (i.e., close or open) of a nanopore in response to a specific stimuli such as a ligand-binding event, a transmembrane potential, or a mechanical force. ¹, ² As a result, the regulation usually causes a transient conformational change in the protein nanopore that can lead to a measurable change in ion permeability across the channel. ³ Due to its nanoscale sized dimension, the protein

nanopore allows the passage of analytes at the single molecule level and accordingly, the changes in ionic currents are commonly representing intermolecular interactions caused by capture or rejection of cargos or transport of molecules.⁴ Hence, protein nanopores can serve as an impressive analytical tool for fundamental and applied science, particularly in fields of biophysics,^{5, 6} and biochemistry.⁷

The alpha-hemolysin (α -HL) protein pore is the most widely used sensing element in the nanopore field due to its various merits such as ultra-sensitivity, selectivity, and stability in severe chemical and physical conditions. ⁸⁻¹⁰ In the past two decades, this protein nanopore has been

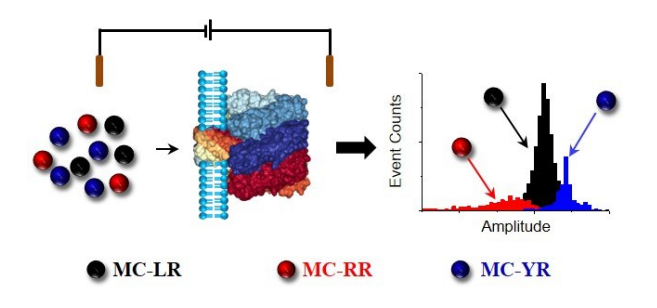
largely utilized to investigate a wide range of biology topics, $^{11-15}$ concentrating on the single molecule study on the basis of favorable and unfavorable intermolecular interactions between biomolecules and the α -HL pore. For instance, our group has carried out a series of studies with both the wild-type α -HL protein and its mutants. Our research effort includes study of ssDNA translocation and dsDNA unzipping, $^{16, 17}$ monitoring proteolysis cleavage, $^{18, 19}$ and probing various chemical reactions such as host-guest, hybridization, chelation, and noncovalent bonding interactions. $^{20-23}$

Since peptide transport is essential to life, peptide-protein pore interactions have attracted substantial interest in the recent years, where the mechanisms of biomolecular interactions were well revealed accordingly.²⁴⁻²⁹ However, in those studies, the majority of the peptide analytes were linear molecules. One concern remains to be resolved: would the transport of cyclic peptides such as nonribosomal peptides (NRPs) in the protein pores use the same molecular interaction mechanism as that involved in the linear peptide transport? NRPs are a group of diverse natural peptides synthesized by nonribosomal peptide synthetases (NRPSs) in microorganisms such as bacteria and fungi.30 In contrast to ribosomal peptides, their structures are totally different. Briefly, there are two significant traits which make them distinguishable from ribosomally synthesized peptides. First is the small cyclic (totally or partially) rather than the traditional linear structure. 31, 32 Second and foremost, NRPs contain not only the common 21 proteinogenic amino acids but also have diverse building blocks including modified amino acids (e.g. methylated, hydroxylated, and D-forms) and other unusual amino acid residues, for example, aminoisobutyric acid (Aib), hydroxyphenylglycine (Hpg), amino-9methoxy-2,6,8-trimethyl-10-phenyl-4,6-decadienoic acid (Adda), N-methyldehydroalanine (MDha), and so on. Hence, compared to normal peptides that rarely exceed 20 components in length, NRPs have much more complicated chemical and structural properties.³³ In addition, since NRPs can interact with a variety of biomolecular targets in

complicated biological processes, their biological effects are numerous as well.^{34, 35} For example, additional NRPs diversification occurs during chain assembly on the NRPs multi-enzyme complex. This diversification usually happens at chain termination step during NRP biosynthesis or at post-assembly-line tailoring reactions (analogous to post-translational modifications, PTMs of ribosomally synthesized peptides).^{36, 37} As a result, these pathways produce a large number of medically relevant compounds,³⁸ which are of great use for antibacterial, immunosuppressant, or anticancer activity, making cyclic NPRs as a unique and extremely selective candidate for biomarker and pharmaceutical screening. Although biochemical and structural studies have uncovered the synthesis mechanism of cyclic NRPs, the mechanism of the intermolecular interaction during the transport of NRPs in the transmembrane protein ion channel remains unclear, which hinders our understanding of NRPs' toxicity to cells.

The present study aims to investigate the biomolecular interaction between NRPs and the protein pore at the single molecule level. Specifically, we use cyclic heptapeptides microcystins (MCs) (Scheme 1), which are derived from cyanobacterial toxins, as model NRPs, to study their transport in the wild-type α-HL protein nanopore. It was previously demonstrated that MCs have tumor promotion effects³⁹ as well as potent inhibition of eukarvotic protein serine/threonine phosphatases in cellular processes.⁴⁰ It was also proposed that the inhibition of protein phosphatases was induced by non-covalent interaction by MCs hydrophobic Adda side-chain and the glutamyl carboxyl after their uptake into hepatocytes via a transport system.41, 42 Our results demonstrated that the intermolecular interaction of MC-α-HL protein was affected by the applied transmembrane potential. The voltage-dependent studies suggested that the biomolecular bumping interaction between MCs and the α-HL protein pore was dominantly contributed by the electrophoretic driven force. Additionally, our results demonstrated that the affinity order of intermolecular interactions between MCs and the α-HL protein pore was MC-YR> MC-LR>

MC-RR, indicating that the net charge and volume of the biomolecule played a significant role in the interaction strength. Our findings should provide an insight in developing a rapid and effective method for the identification of cyclic NRPs as valuable biomarkers for antifungal infections in the pharmaceutical industry.



Scheme 1. Detection of cyclic heptapeptides microcystins in a nanopore platform.

2. Material and Methods

2.1. Materials and reagents

Microcystins were purchased from Puhuashi Technology Development Co., Ltd. (Beijing, China). MC-LR linear analog (D- τ -Glu-L-Ala-D-Ala-L-Leu-D-Asp-L-Arg-L-Tyr) was synthesized and purified by ChinaPeptides Co., Ltd. (Shanghai, China). The wild-type alpha-hemolysin and other chemicals including NaCl and Trizma base were purchased from Sigma-Aldrich (St. Louis, MO, USA). The electrolyte solution was composed of 3.0/1.0/0.5 M NaCl and 10 mM Tris, with the solution pH adjusted to 7.5. The stock solutions of MC-LR, MC-RR and MC-YR were prepared at 200 μ g/mL, 1 μ g/mL, and 0.25 μ g/mL, respectively, and kept at -20°C before and after use. All of the solutions were prepared with ultrapure water from a water purification system (Molecular 1850D).

2.2. Single-molecule Study

The nanopore electrical recording was conducted based on our previous report.¹⁸ Briefly, according to the Montal-Mueller method,⁴³ a planar lipid bilayer using 1, 2-

diphytanoylphosphatidylcholine (Avanti Polar Lipids, Alabaster, AL) was formed on a 150 μ m aperture of a Teflon film which separated the experimental chamber into two compartments (cis and trans). Unless otherwise noted, all the experiments were carried out at 20 \pm 1 °C under symmetrical buffer solutions with both the compartments filled with a 1.5 mL electrolyte solution comprising 1 M NaCl and 10 mM Tris·HCl (pH 7.5), where the NRPs peptide analytes were added to the trans chamber compartment, while the wild-type α -HL protein pore was added to the cis compartment.

Simulated MC-LR contaminating water samples were prepared by spiking MC-LR (with concentrations of 15 mg/L) into 20- μ L of tap water, bottle water and Yangtze River water). Then, these water samples (with final concentrations of 200 μ g/L each) were introduced to the *trans* chamber compartment of the nanopore sensing device for MC-LR testing.

2.3. Data Acquisition and Analysis

The current traces were recorded on a patch-clamp amplifier (Axopatch 200B, Molecular Devices, USA). The signal was sampled at 20 kHz and low-pass filtered at 5 kHz through the Clampex 10.6 software. All the experimental data were analyzed by using Clampfit 10.4 and Origin 8.6.0.

3. Results and discussions

3.1. Determination of the Intermolecular Interaction between Cyclic NRPs and the α-HL protein pore

With microcystins as model NRPs, we, for the first time, determined the interaction between cyclic NRPs and the wild-type α -HL protein nanopore. As illustrated in Figure 1A, structurally, microcystins are monocyclic heptapeptides with approximately \sim 3 nm in diameter. These cyclic NRPs are composed of three unusual amino acids (MeAsp, Adda and MDha), one D-alanine, one g-

linked D-glutamic acid and two variable L-amino acids. 40 In this work, MC-LR, the most common structural variant of over 50 different microcystins was used as the model cyclic NRPs, where the two variable L-amino acids are leucine (L) and arginine (R), respectively. As to the protein nanopore, it is well known that wild-type alpha-hemolysin can form a mushroom-shaped heptameric transmembrane channel by seven self-assembling identical subunits that are embedded into the planar lipid bilayer. 8 This protein nanopore is around 10 nm in length. The openings of its cis and trans ends are ~2.9 nm and ~2.0 nm, respectively, while its constriction area is only about 1.4 nm in diameter (Figure 1B). Hence, due to its larger size, the MC-LR molecule (Figure 1b) is hardly able to traverse through the wild-type α-HL protein channel. However, it is likely that the intermolecular interaction between the MC-LR molecule and the α -HL pore at its *cis* / *trans* entrance might induce current modulation events under an applied electric field.

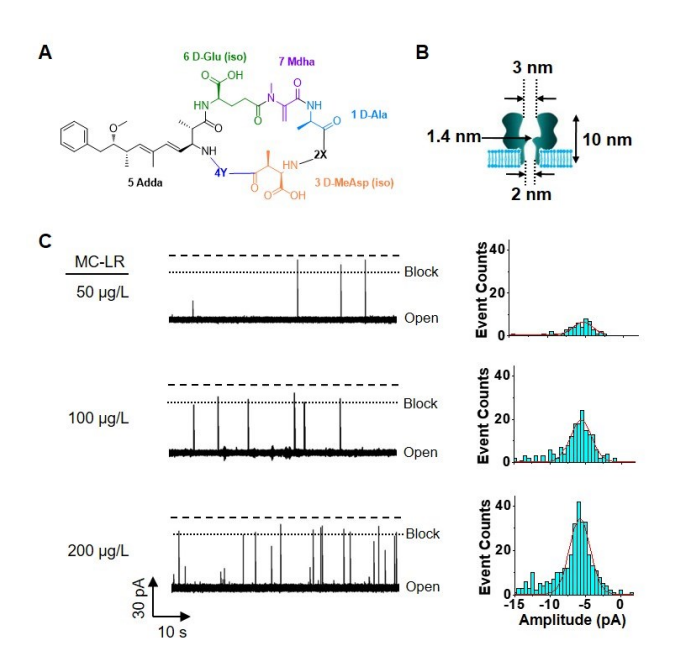


Figure 1. Detection of microcystins in the α-hemolysin pore. (A) The chemical structure of microcystins, in which the amino acid residues at position 2 (X) and 4 (Y) are Leu (L) and Arg (R) for MC-LR, Arg (R) and Arg (R) for MC-RR, Tyr (Y) and Arg (R) for MC-YR, respectively;

(B) the schematic illustration of the α -hemolysin protein supported by a planar lipid bilayer; and (C) typical single-channel recording trace segments and their corresponding amplitude histograms of MC-LR at various concentrations. Dashed lines represent the levels of zero current. The experiments were performed at -80 mV with the wild-type α -hemolysin pore in a solution comprising 1 M NaCl and 10 mM Tris•HCl (pH7.5). Traces were filtered at 2 kHz for display purpose.

As a proof-of-concept purpose, the intermolecular interaction was initially investigated under a combination of various experimental conditions. These included the effects of the polarity (positive vs. negative) and value (ranging from 60 to 100 mV) of the applied potential bias across the nanopore as well as the effect of cis-trans analyte addition. As shown in Figure S1, when MC-LR was added to the cis side of the α-HL channel, current modulation events were seldom observed no matter whether a positive voltage or a negative potential was applied, indicating the weak or no biomolecular interaction between MC-LR and the α-HL protein pore. Note that, at pH 7.5, the MC-LR molecule has two COO groups and one NH₂⁺ group in the electrolyte solution (Table S1), and hence it has a net negative charge, thus favoring its weak interaction with the α-HL protein when negative voltages were applied. Although, at an applied positive voltage, the interaction between the α-HL protein pore and negatively charged MC-LR would produce more frequent current modulation events due to the electrophoretic driven force, the strong electric field would lead to the instability of the planar lipid bilayer. On the other hand, when MC-LR was added to the trans reservoir, much more frequent current modulation events were observed at negatively applied voltages compared to positively applied potentials. This is not unreasonable considering that the negatively charged MC-LR molecule would be subjected electrophoretic driven force and hence interacted with the protein pore, subsequently leading to the generation of current modulation events. To confirm that these events were attributed to the intermolecular interaction between MC-LR and the α -HL pore, the effect of MC-LR concentration on the event frequency was further investigated. Our results (Figure 1C and Figure S2) showed that, with an increase in the added MC-LR concentration, more frequent current modulation events were observed. The linear dose-response curve for MC-LR in the α -HL pore supported the interpretation that these events were indeed due to the intermolecular interaction between MC-LR and the α -HL protein.

3.2. Voltage-dependent and Salt Gradient Studies on the Interaction between NRPs and the α-HL channel

To find an optimum experimental condition for the investigation of the intermolecular interaction between MC-LR and the α -HL pore, the voltage-dependent study was then conducted in detail. As shown in Figure 2A, with an increase in the applied voltage bias, the blockage amplitude of the current modulations showed no significant difference, indicating that the observed events were dominantly contributed to the bumping interaction between MC-LR and the α-HL protein via the electrophoretic force. Furthermore, we found that the mean residence time of the bumping events exhibited a two-stage decrease (from 1.90 ms to 1.02 ms, and from 1.02 ms to 0.69 ms) at the threshold voltages of -70 mV and -100 mV, respectively (Figure 2B). One likely interpretation lies in the two energy barriers at the trans entrance of the nanochannel that the MC-LR molecules had to overcome in order for them to interact with the α-HL protein (i.e., MC-LR passed from the free aqueous electrolyte solution in the trans compartment to the binding site within the α-HL channel, and returned from the binding site of the α-HL nanopore to the trans solution). Our finding is in good agreement with the previous study on the hydrogen bond interaction between a single oligonucleotide molecule and the aerolysin nanopore.⁴⁴ Taken together, our results demonstrated that the intermolecular interaction of MC-α-HL protein was affected by the applied potential bias. A voltage of -80 mV was chosen as the optimum applied potential and used in the remaining experiments since a good nanopore resolution/performance was achieved at this voltage bias.

In addition to the voltage effect, an asymmetric salt gradient is often used in the nanopore field to enhance the electro-osmotic flow and to increase the biomolecule capture rate, thus increasing the nanopore sensor sensitivity. 45,46 For this purpose, a salt gradient of 3 M NaCl (trans) / 0.5 M NaCl (cis) was utilized to investigate the intermolecular interaction between MC-LR and the α -HL protein pore. Unlike the significantly (~100 to 1000 folds) increased ssDNA capture rate reported in the previous studies on DNA translocation in the nanopore, 47 our experiment (Figure 2C) showed that the event frequency for MC-LR in the α-HL protein pore obtained under the asymmetric electrolyte condition was only slightly (1.55 fold) larger than that with the symmetric electrolyte solution. The results gave further evidence that the events induced by the interaction between MC-LR and the α -HL protein was likely due to collision instead of translocation.

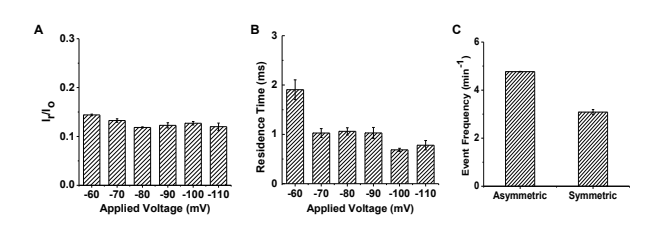


Figure 2. The effect of experimental conditions on the resolution and performance of the wild-type α-hemolysin pore. Plots of (A) event blockage amplitude and (B) mean residence time of MC-LR vs. applied potential bias; and (C) salt gradient effect on MC-LR event frequency. I_r/I_o in Figure 2A is normalized blockage residual current, which was obtained by dividing the average blockage residual current of an event by the average open channel current. The experiments described in Figure 2A, Figure 2B, and Figure 2C (symmetric) were performed in a solution comprising 1 M NaCl and 10 mM Tris \bullet HCl (pH7.5), while the asymmetric electrolyte experiment shown in Figure 2C was carried out in a salt gradient of 3 M NaCl (*trans*) / 0.5

M NaCl (*cis*). The concentration of MC-LR used in Figures 2A and 2B was 250 μ g/L, while that of Figure 2C was 100 μ g/L. The applied voltage in Figure 2C was -80 mV.

3.3. Discrimination of NRPs Variants via Intermolecular Interaction

Thus far, there are more than 50 variants in the family of microcystins. 48 Although they share the same basic cyclic peptide structure, different types of microcystins have different toxicities. Therefore, it is of great importance to have analytical capacity to differentiate them. To this end, we investigated the feasibility of utilizing the biomolecular interaction of MC-α-HL protein pore to discriminate MCs variants. For proof-of-concept demonstration, 3 types of microcystins, including MC-RR, MC-LR and MC-YR, were examined. All the three MCs belong to the cyclic NRPs with similar cyclic structures but having a different polarity L- amino acid. The variable L-amino acid in the other two MCs are positively charged arginine (R) and aromatic Tyrosine (Y) residues, respectively. Note that, since the pKa values of arginine, leucine and tyrosine are 10.76, 6.01 and 5.64, respectively, they should possess different net charges in the electrolyte solution at pH 7.5. Among them, MC-RR has a zero net charge, while both MC-LR and MC-YR are carrying one negative charge. Therefore, their interaction affinity with the α -HL protein pore should be different. The experimental results (scatter plot of event residence time vs. blockage amplitude, amplitude histogram, and the mean event residence time and amplitude) were summarized in Figure 3 and Supporting Information, Figure S3 and Table S2, respectively. It was apparent that both MC-LR and MC-YR showed much larger residence time than MC-RR $(1.02\pm0.08 \text{ ms} \text{ and } 2.08\pm0.13 \text{ ms vs. } 0.37\pm0.04 \text{ ms}),$ indicating their stronger molecular interactions. As to the event amplitude, MC-YR produced the smallest residual current (-5.78±0.04 pA) and hence the largest blockage among the three variants. The result is in agreement with the fact that tyrosine has the largest volume among the

three amino-acids (V_Y, V_R, and V_L are 193.6 Å³, 173.4 Å³, and 166.7 Å³, respectively).⁴⁹ Interestingly, we also noticed that, although lecine has a smaller volume than arginine, MC-LR showed a larger blockage amplitude than MC-RR (residual currents: -8.66±0.02 pA vs. -13.11±0.10 pA). The result suggested that, in addition to the molecular size, the structure and the charge of the analyte molecule also played a role in the event blockage amplitude. Since MC-LR, MC-YR, and MC-RR produced events with significantly different residence time and blockage amplitude values, these three microcystins could be readily differentiated from each other and even simultaneously detected (Figure 3). Taken together, our experimental results showed that, under the electrophoretic driven force, the affinity order of intermolecular interactions between MCs and the α-HL protein pore was MC-YR> MC-LR> MC-RR.

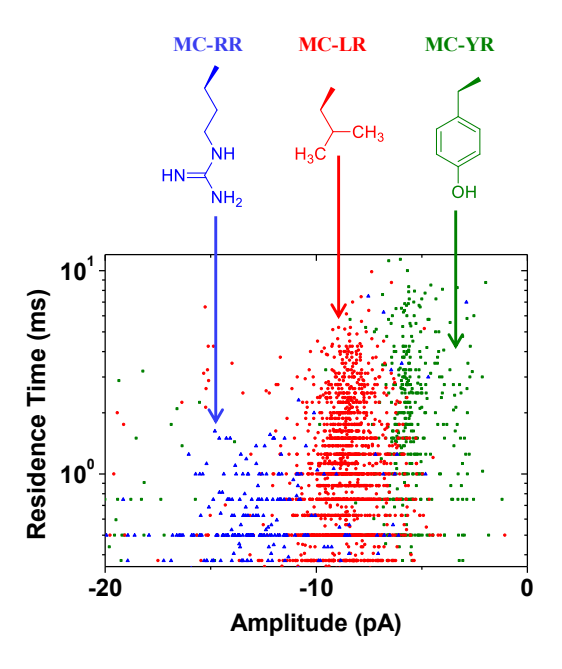


Figure 3. Scatter plots of event residence time vs. residual current for MC-RR, MC-LR and MC-YR in the wild-type α-hemolysin pore, showing the discrimination of three types of microcystins via MC/α-HL interaction under an electrophoretic driven force. The experiments were performed at -80 mV in a solution comprising 1 M NaCl and 10 mM Tris•HCl (pH7.5). The concentrations of MC-

3.4. Discrimination of Cyclic NRPs and their Linear Analog via Tryptic-digestion

Besides discrimination of cyclic NRPs structural variants, differentiation of cyclic NRPs from their linear analog is also desirable. For this purpose, another experiment was carried out, where the interactions between MC-LR / its linear analog (with their chemical structures shown in the Supporting Information, Figure S4) and the α-HL protein pore were investigated in the presence of trypsin, a serine protease, which is able to cleave the peptide bonds containing lysine (K) and arginine (R) residue. Note that, one of the reasons of utilizing cyclic NRPs as fungal biomarkers is due to their great biochemical stability. Most cyclic NRPs are not amenable to proteolytic cleavage. The experimental results were summarized in Figure 4. We could see that no new types of events appeared in the current trace after addition of trypsin to the MC-LR containing solution, supporting our prediction that MC-LR could not be cleaved by trypsin. In contrast, the interaction between the MC-LR linear analog and the αhemolysin pore rarely produced characteristic current modulations in the absence of trypsin, but generated frequent short-lived blockage events (due to the short peptide cleavage fragments) in the presence of trypsin. In addition to discriminating between MC-LR and its linear analogue based on their quite different responses toward tryptic digestion, these two species could also be readily differentiated from their different event signatures. Specifically, in the presence of trypsin, MC-LR produced much larger residence time and blockage amplitude events in the α-HL protein pore than its linear analog (Figure 4A and 4B).

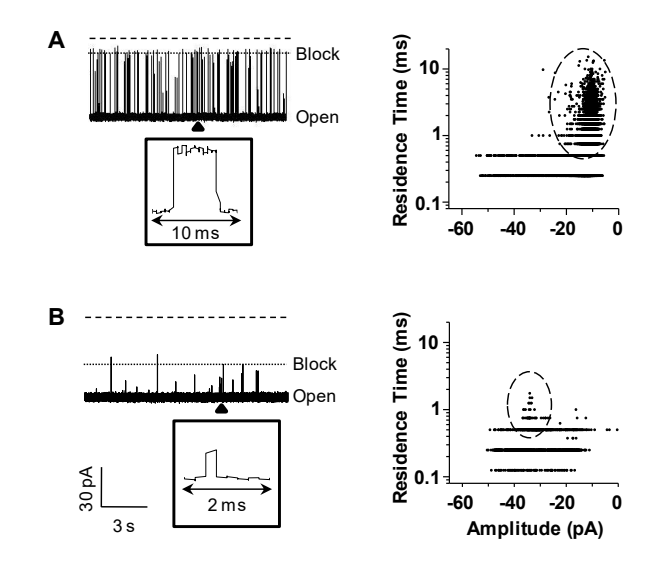


Figure 4. Differentiation of (A) cyclic MC-LR and (B) its linear analog via tryptic-digestion. (*Left*) Typical single-channel recording trace segments. Dashed lines represent the levels of zero current. Insets show enlarged images of arrow-marked events; and (*Right*) the corresponding scatter plots of event residence time vs. residual current. The experiments were performed at -80 mV with the wild-type α-hemolysin pore in a solution comprising 1 M NaCl and 10 mM Tris•HCl (pH7.5). The concentrations of MC-LR and its linear analog were 3.98 mg/L and 3.35 mg/L, respectively, while the concentration of trypsin was 150 ng/mL.

Finally, to show its real-world applications, three simulated water samples were analyzed based on our developed MC- α -HL interaction strategy. These samples were prepared by spiking tap water, bottle water, and Yangzte River water with 200 μ g/L of MC-LR. Our results (Supporting Information, Figure S5) demonstrated that the various matrix components in the water samples would not interfere with MC-LR detection significantly.

4. Conclusions

In summary, by monitoring the current modulations induced by the movement of MCs in the α -HL pore, we studied the intermolecular interaction between MCs and

the biological protein. As far as we are aware, this is the first time to investigate the intermolecular interaction between a protein ion channel and cyclic nonribosomal peptides at the single molecule level. Our experimental results showed that the current modulation events were dominantly caused by the bumping interactions between the cyclic NRPs and the α -HL protein pore. Furthermore, the biomolecular interaction of MC-α-HL protein was affected by the applied potential bias. Using the MC-α-HL protein interaction strategy, discrimination of MC variants (MC-LR, MC-RR, MC-YR and their linear analogs) with varied branched residues and structures could be readily accomplished. Our results also demonstrated that the affinity order of intermolecular interactions between MCs and the α-HL protein pore was MC-YR> MC-LR> MC-RR, indicating that both the net charge and the volume of the biomolecule played a significant role in the interaction strength. In addition, MCs were successfully detected in various simulated water samples. This work should provide an insight in developing rapid and effective methods for the identification of cyclic NRPs as valuable biomarkers for fungal infections.

ASSOCIATED CONTENT

Supporting Information.

The Supporting Information is available free of charge on the ACS Publications website.

Additional figures and tables, including typical 100-s single channel recording trace segments of MC-LR in the α -HL pore at various applied voltages, the plot of event frequency as a function of MC-LR concentration, differentiation of three types of MCs via amplitude histograms, chemical structures of MC-LR and its linear analog, determination of MC-LR in simulated water samples with the α -HL protein nanopore, dominant functional groups and net charges of MCs at pH 7.5, and event mean residence time and blockage residual current of MCs.

AUTHOR INFORMATION

Corresponding author

*Tel: 312-567-8922. Fax: 312-567-3494.

E-mail: wangliang83@cigit.ac.cn (Liang Wang);

dqwang@cigit.ac.cn (Deqiang Wang);

xguan5@iit.edu(Xiyun Guan).

Notes

The authors declare no competing financial interests.

ACKNOWLEDGMENT

We gratefully thank the National Natural Science Foundation of China (31800711, 61701474), National Institutes of Health (2R15GM110632-02), National Science Foundation (1708596), West Light Foundation of CAS, and the Youth Innovation Promotion Association of CAS (2017392) to support this work. In addition, Liang Wang is also sponsored by Pioneer Hundred Talents Program of Chinese Academy of Sciences (CAS); Natural Foundation Science of Chongqing, China (cstc2018jcyjAX0304); the Entrepreneurship and Innovation Support Program for Returned Oversea Students of Chongqing, China (cx2018156).

Reference

- (1) Majd, S.; Yusko, E. C.; Billeh, Y. N.; Macrae, M. X.; Yang, J.; Mayer, M. Applications of Biological Pores in Nanomedicine, Sensing, and Nanoelectronics. Curr. Opin. Biotechnol. 2010, 21 (4), 439–476. https://doi.org/10.1016/j.copbio.2010.05.002.
- (2) Hamill, O. P.; Martinac, B. Molecular Basis of Mechanotransduction in Living Cells. Physiol. Rev. 2001, 81 (2), 685–740. https://doi.org/10.1152/physrev.2001.81.2.685.
- (3) Molecular Biology of the Cell, 4th ed.; Alberts, B., Ed.; Garland Science: New York, 2002.
- (4) Bayley, H.; Cremer, P. S. Stochastic Sensors Inspired

- by Biology. Nature 2001, 413 (6852), 226–230. https://doi.org/10.1038/35093038.
- (5) Jou, I.; Muthukumar, M. Effects of Nanopore Charge Decorations on the Translocation Dynamics of DNA. Biophys. J. 2017, 113 (8), 1664–1672. https://doi.org/10.1016/j.bpj.2017.08.045.
- (6) Bates, M.; Burns, M.; Meller, A. Dynamics of DNA Molecules in a Membrane Channel Probed by Active Control Techniques. Biophys. J. 2003, 84 (4), 2366–2372. https://doi.org/10.1016/S0006-3495(03)75042-5.
- (7) Hurt, N.; Wang, H.; Akeson, M.; Lieberman, K. R. Specific Nucleotide Binding and Rebinding to Individual DNA Polymerase Complexes Captured on a Nanopore. J. Am. Chem. Soc. 2009, 131 (10), 3772–3778. https://doi.org/10.1021/ja809663f.
- (8) Song, L.; Hobaugh, M. R.; Shustak, C.; Cheley, S.; Bayley, H.; Gouaux, J. E. Structure of Staphylococcal Alpha-Hemolysin, a Heptameric Transmembrane Pore. Science 1996, 274 (5294), 1859–1866. https://doi.org/10.1126/science.274.5294.1859.
- (9) Kasianowicz, J. J.; Brandin, E.; Branton, D.; Deamer, D. W. Characterization of Individual Polynucleotide Molecules Using a Membrane Channel. Proc. Natl. Acad. Sci. U.S.A. 1996, 93 (24), 13770–13773. https://doi.org/10.1073/pnas.93.24.13770.
- (10) Wang, H.; Ettedgui, J.; Forstater, J.; Robertson, J. W. F.; Reiner, J. E.; Zhang, H.; Chen, S.; Kasianowicz, J. J. Determining the Physical Properties of Molecules with Nanometer-Scale Pores. ACS Sens 2018, 3 (2), 251–263. https://doi.org/10.1021/acssensors.7b00680.
- (11) Howorka, S. Building Membrane Nanopores. Nat Nanotechnol 2017, 12 (7), 619–630. https://doi.org/10.1038/nnano.2017.99.
- (12) Ayub, M.; Hardwick, S. W.; Luisi, B. F.; Bayley, H. Nanopore-Based Identification of Individual Nucleotides for Direct RNA Sequencing. Nano Lett. 2013, 13 (12), 6144–6150. https://doi.org/10.1021/nl403469r.
- (13) Noakes, M. T.; Brinkerhoff, H.; Laszlo, A. H.; Derrington, I. M.; Langford, K. W.; Mount, J. W.; Bowman, J. L.; Baker, K. S.; Doering, K. M.; Tickman, B. I.; Gundlach, J. H. Increasing the Accuracy of Nanopore

- DNA Sequencing Using a Time-Varying Cross Membrane Voltage. Nat. Biotechnol. 2019, 37 (6), 651–656. https://doi.org/10.1038/s41587-019-0096-0.
- (14) Wang, G.; Wang, L.; Han, Y.; Zhou, S.; Guan, X. Nanopore Stochastic Detection: Diversity, Sensitivity, and Beyond. Acc. Chem. Res. 2013, 46 (12), 2867–2877. https://doi.org/10.1021/ar400031x.
- (15) Kukwikila, M.; Howorka, S. Nanopore-Based Electrical and Label-Free Sensing of Enzyme Activity in Blood Serum. Anal. Chem. 2015, 87 (18), 9149–9154. https://doi.org/10.1021/acs.analchem.5b01764.
- (16) de Zoysa, R. S. S.; Jayawardhana, D. A.; Zhao, Q.; Wang, D.; Armstrong, D. W.; Guan, X. Slowing DNA Translocation through Nanopores Using a Solution Containing Organic Salts. J Phys Chem B 2009, 113 (40), 13332–13336. https://doi.org/10.1021/jp9040293.
- (17) Liu, A.; Zhao, Q.; Krishantha, D. M. M.; Guan, X. Unzipping of Double-Stranded DNA in Engineered α-Hemolysin Pores. J Phys Chem Lett 2011, 2 (12), 1372–1376. https://doi.org/10.1021/jz200525v.
- (18) Wang, L.; Han, Y.; Zhou, S.; Guan, X. Real-Time Label-Free Measurement of HIV-1 Protease Activity by Nanopore Analysis. Biosens Bioelectron 2014, 62, 158–162. https://doi.org/10.1016/j.bios.2014.06.041.
- (19) Chen, X.; M Roozbahani, G.; Ye, Z.; Zhang, Y.; Ma, R.; Xiang, J.; Guan, X. Label-Free Detection of DNA Mutations by Nanopore Analysis. ACS Appl Mater Interfaces 2018, 10 (14), 11519–11528. https://doi.org/10.1021/acsami.7b19774.
- (20) Jayawardhana, D. A.; Crank, J. A.; Zhao, Q.; Armstrong, D. W.; Guan, X. Nanopore Stochastic Detection of a Liquid Explosive Component and Sensitizers Using Boromycin and an Ionic Liquid Supporting Electrolyte. Anal. Chem. 2009, 81 (1), 460–464. https://doi.org/10.1021/ac801877g.
- (21) Wang, L.; Han, Y.; Zhou, S.; Wang, G.; Guan, X. Nanopore Biosensor for Label-Free and Real-Time Detection of Anthrax Lethal Factor. ACS Appl Mater Interfaces 2014, 6 (10), 7334–7339. https://doi.org/10.1021/am500749p.
- (22) Wang, G.; Zhao, Q.; Kang, X.; Guan, X.

- Probing Mercury(II)-DNA Interactions by Nanopore Stochastic Sensing. J Phys Chem B 2013, 117 (17), 4763–4769. https://doi.org/10.1021/jp309541h.
- (23) Zhao, Q.; Jayawardhana, D. A.; Guan, X. Stochastic Study of the Effect of Ionic Strength on Noncovalent Interactions in Protein Pores. Biophys. J. 2008, 94 (4), 1267–1275. https://doi.org/10.1529/biophysj.107.117598.
- (24) Zhao, Q.; de Zoysa, R. S. S.; Wang, D.; Jayawardhana, D. A.; Guan, X. Real-Time Monitoring of Peptide Cleavage Using a Nanopore Probe. J. Am. Chem. Soc. 2009, 131 (18), 6324–6325. https://doi.org/10.1021/ja9004893.
- (25) Zhao, Q.; Jayawardhana, D. A.; Wang, D.; Guan, X. Study of Peptide Transport through Engineered Protein Channels. J Phys Chem B 2009, 113 (11), 3572–3578. https://doi.org/10.1021/jp809842g.
- (26) Luchian, T.; Park, Y.; Asandei, A.; Schiopu, I.; Mereuta, L.; Apetrei, A. Nanoscale Probing of Informational Polymers with Nanopores. Applications to Amyloidogenic Fragments, Peptides, and DNA-PNA Hybrids. Acc. Chem. Res. 2019, 52 (1), 267–276. https://doi.org/10.1021/acs.accounts.8b00565.
- (27) Chavis, A. E.; Brady, K. T.; Hatmaker, G. A.; Angevine, C. E.; Kothalawala, N.; Dass, A.; Robertson, J. W. F.; Reiner, J. E. Single Molecule Nanopore Spectrometry for Peptide Detection. ACS Sens 2017, 2 (9), 1319–1328. https://doi.org/10.1021/acssensors.7b00362.
- (28) Asandei, A.; Chinappi, M.; Lee, J.-K.; Ho Seo, C.; Mereuta, L.; Park, Y.; Luchian, T. Placement of Oppositely Charged Aminoacids at a Polypeptide Termini Determines the Voltage-Controlled Braking of Polymer Transport through Nanometer-Scale Pores. Sci Rep 2015, 5, 10419. https://doi.org/10.1038/srep10419.
- (29) Lee, J. S. Nanopore Analysis of the Effect of Metal Ions on the Folding of Peptides and Proteins. Protein Pept. Lett. 2014, 21 (3), 247–255. https://doi.org/10.2174/09298665113209990075.
- (30) Gewolb, J. Bioengineering. Working Outside the Protein-Synthesis Rules. Science 2002, 295 (5563), 2205–2207.

- https://doi.org/10.1126/science.295.5563.2205.
- (31) Blout, E. R. Cyclic Peptides: Past, Present, and Future. Biopolymers 1981, 20 (9), 1901–1912. https://doi.org/10.1002/bip.1981.360200913.
- (32) Crawford, J. L.; Lipscomb, W. N.; Schellman, C. G. The Reverse Turn as a Polypeptide Conformation in Globular Proteins. Proc. Natl. Acad. Sci. U.S.A. 1973, 70 (2), 538–542. https://doi.org/10.1073/pnas.70.2.538.
- (33) Pupin, M.; Esmaeel, Q.; Flissi, A.; Dufresne, Y.; Jacques, P.; Leclère, V. Norine: A Powerful Resource for Novel Nonribosomal Peptide Discovery. Synth Syst Biotechnol 2016, 1 (2), 89–94. https://doi.org/10.1016/j.synbio.2015.11.001.
- (34) Keller, N. P.; Turner, G.; Bennett, J. W. Fungal Secondary Metabolism from Biochemistry to Genomics. Nat. Rev. Microbiol. 2005, 3 (12), 937–947. https://doi.org/10.1038/nrmicro1286.
- (35) Biotechnology: A Multi-Volume Comprehensive Treatise, 2nd ed.; Rehm, H.-J., Reed, G., Eds.; Wiley VCH: Weinheim, 1999.
- (36) Grünewald, J.; Marahiel, M. A. Nonribosomal Peptide Synthesis. In Handbook of Biologically Active Peptides; Elsevier, 2013; pp 138–149. https://doi.org/10.1016/B978-0-12-385095-9.00021-X.
- (37) Walsh, C. T.; Chen, H.; Keating, T. A.; Hubbard, B. K.; Losey, H. C.; Luo, L.; Marshall, C. G.; Miller, D. A.; Patel, H. M. Tailoring Enzymes That Modify Nonribosomal Peptides during and after Chain Elongation on NRPS Assembly Lines. Curr Opin Chem Biol 2001, 5 (5), 525–534.
- (38) Süssmuth, R. D.; Mainz, A. Nonribosomal Peptide Synthesis-Principles and Prospects. Angew. Chem. Int. Ed. Engl. 2017, 56 (14), 3770–3821. https://doi.org/10.1002/anie.201609079.
- (39) Nishiwaki-Matsushima, R.; Ohta, T.; Nishiwaki, S.; Suganuma, M.; Kohyama, K.; Ishikawa, T.; Carmichael, W. W.; Fujiki, H. Liver Tumor Promotion by the Cyanobacterial Cyclic Peptide Toxin Microcystin-LR. Journal of Cancer Research and Clinical Oncology 1992, 118 (6), 420–424. https://doi.org/10.1007/BF01629424.
- (40) Dawson, R. M. The Toxicology of Microcystins.

- Toxicon 1998, 36 (7), 953–962. https://doi.org/10.1016/s0041-0101(97)00102-5.
- (41) An, J.; Carmichael, W. W. Use of a Colorimetric Protein Phosphatase Inhibition Assay and Enzyme Linked Immunosorbent Assay for the Study of Microcystins and Nodularins. Toxicon 1994, 32 (12), 1495–1507. https://doi.org/10.1016/0041-0101(94)90308-5.
- (42) Honkanen, R. E.; Zwiller, J.; Moore, R. E.; Daily, S. L.; Khatra, B. S.; Dukelow, M.; Boynton, A. L. Characterization of Microcystin-LR, a Potent Inhibitor of Type 1 and Type 2A Protein Phosphatases. J. Biol. Chem. 1990, 265 (32), 19401–19404.
- (43) Montal, M.; Mueller, P. Formation of Bimolecular Membranes from Lipid Monolayers and a Study of Their Electrical Properties. Proc. Natl. Acad. Sci. U.S.A. 1972, 69 (12), 3561–3566. https://doi.org/10.1073/pnas.69.12.3561.
- (44) Li, M.-Y.; Wang, Y.-Q.; Lu, Y.; Ying, Y.-L.; Long, Y.-T. Single Molecule Study of Hydrogen Bond Interactions Between Single Oligonucleotide and Aerolysin Sensing Interface. Front Chem 2019, 7, 528. https://doi.org/10.3389/fchem.2019.00528.
- (45) Mereuta, L; Asandei, A.; Seo, C. H.; Park, Y.; Luchian, T. Quantitative Understanding of pH- and Salt-Mediated

Conformational Folding of Histidine-Containing, · β-

Hairpin-like Peptides, Through Single-Molecule Probing with Protein Nanopores. ACS Applied Materials &

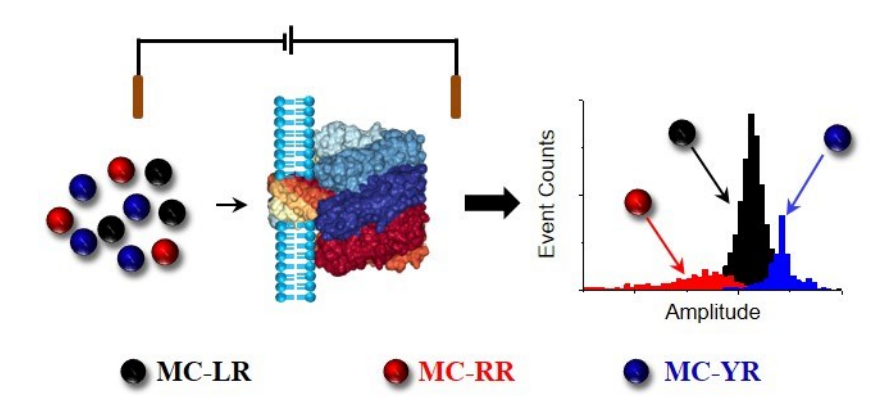
Interfaces 2014, 6, 13242 - 13256.

https://doi.org/10.1021/am5031177

- (46) Mereuta, L; Asandei, A.; Schiopu, I.; Park, Y.; Luchian, T. Nanopore-Assisted, Sequence-Specific Detection and Single-Molecule Hybridization Analysis of Short, Single-Stranded DNAs, Analytical Chemistry 2019, https://doi.org/10.1021/acs.analchem.9b02080
- (45) Ivica, J.; Williamson, P. T. F.; de Planque, M. R. R. Salt Gradient Modulation of MicroRNA Translocation through a Biological Nanopore. Anal. Chem. 2017, 89 (17), 8822–8829.

https://doi.org/10.1021/acs.analchem.7b01246.

- (48) Bortoli, S.; Volmer, D. A. Account: Characterization and Identification of Microcystins by Mass Spectrometry. Eur J Mass Spectrom (Chichester) 2014, 20 (1), 1–19.
- (49) Zamyatnin, A. A. Protein Volume in Solution. Prog. Biophys. Mol. Biol. 1972, 24, 107–123.



Scheme 1. Detection of cyclic heptapeptides microcystins in a nanopore platform.

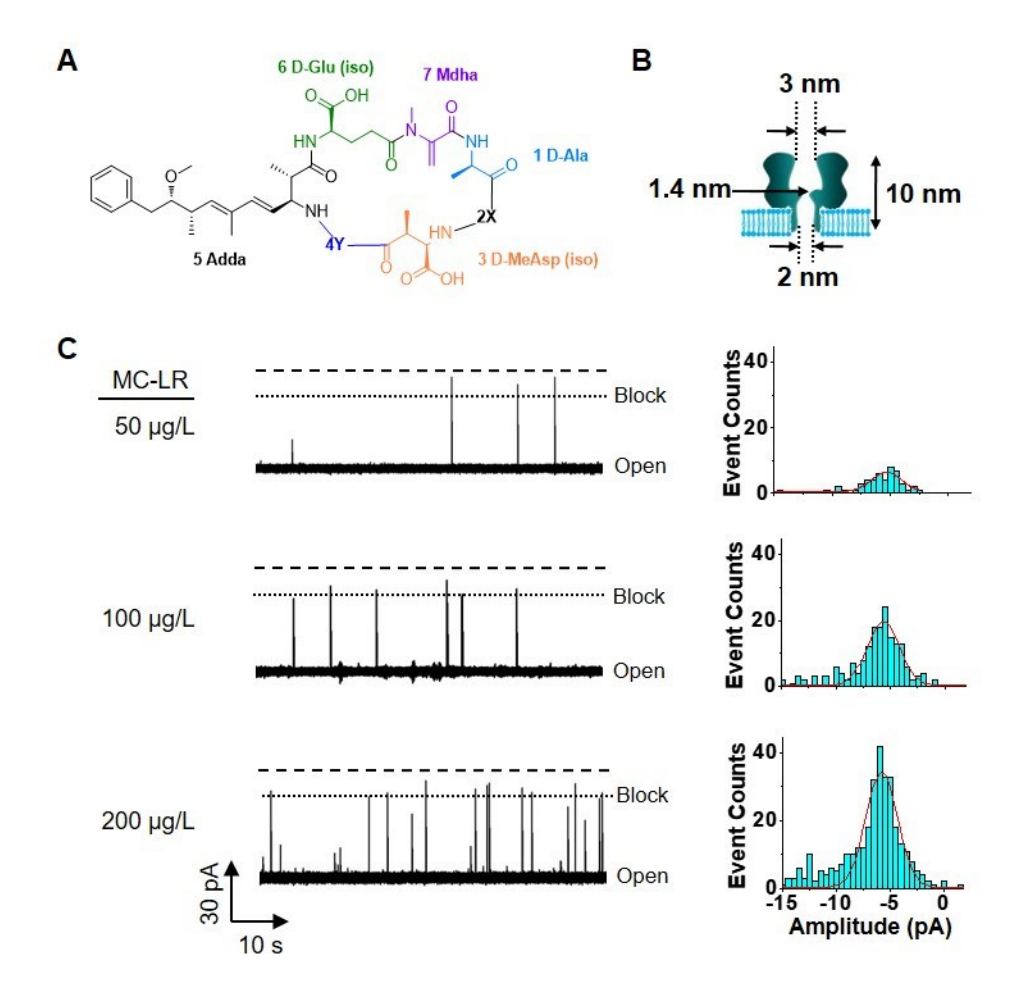


Figure 1. Detection of microcystins in the α -hemolysin pore. (A) The chemical structure of microcystins, in which the amino acid residues at position 2 (X) and 4 (Y) are Leu (L) and Arg (R) for MC-LR, Arg (R) and Arg (R) for MC-RR, Tyr (Y) and Arg (R) for MC-YR, respectively; (B) the schematic illustration of the α -hemolysin protein supported by a planar lipid bilayer; and (C) typical single-channel recording trace segments and their corresponding amplitude histograms of MC-LR at various concentrations. Dashed lines represent the levels of zero current. The experiments were performed at -80 mV with the wild-type α -hemolysin pore in a solution comprising 1 M NaCl and 10 mM Tris \bullet HCl (pH7.5). Traces were filtered at 2 kHz for display purpose.

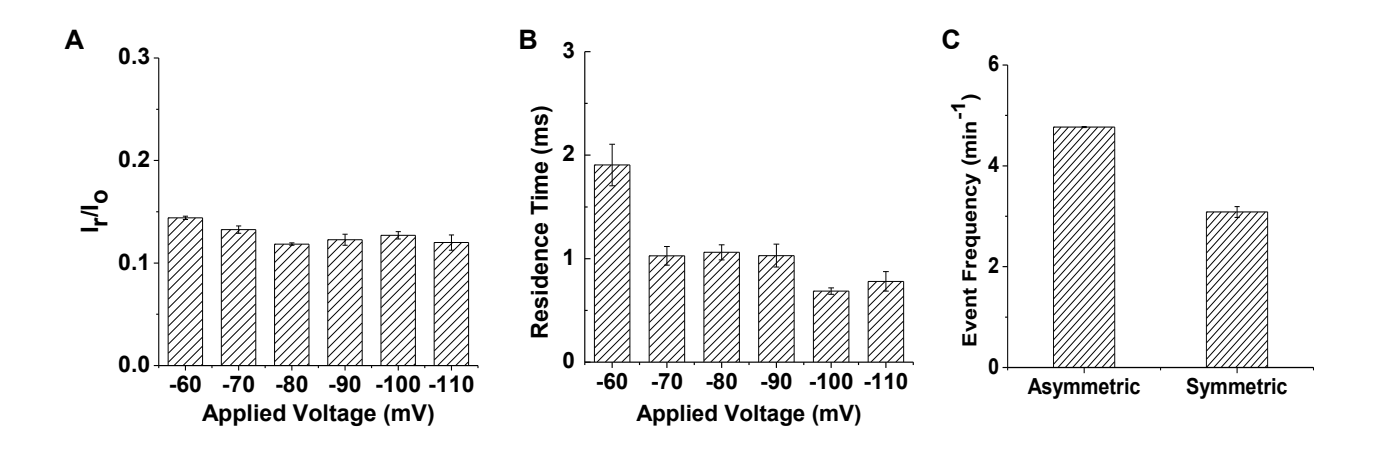


Figure 2. The effect of experimental conditions on the resolution and performance of the wild-type α-hemolysin pore. Plots of (A) event blockage amplitude and (B) mean residence time of MC-LR vs. applied potential bias; and (C) salt gradient effect on MC-LR event frequency. The experiments described in Figure 2a, Figure 2b, and Figure 2c (symmetric) were performed in a solution comprising 1 M NaCl and 10 mM Tris•HCl (pH7.5), while the asymmetric electrolyte experiment shown in Figure 2c was carried out in a salt gradient of 3 M NaCl (trans) / 0.5 M NaCl (cis). The concentration of MC-LR used in Figures 2a and 2b was 250 μg/L, while that of Figure 2c was 100 μg/L. The applied voltage in Figure 2c was -80 mV.

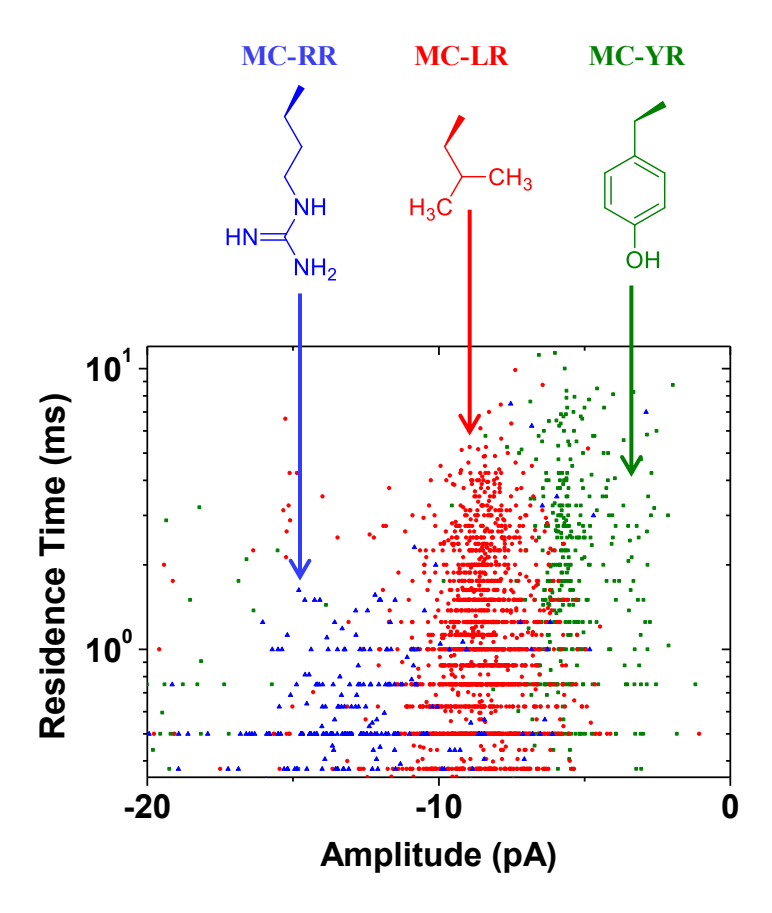


Figure 3. Scatter plots of event residence time vs. residual current for MC-RR, MC-LR and MC-YR in the wild-type α-hemolysin pore, showing the discrimination of three types of microcystins via MC/α-HL interaction under an electrophoretic driven force. The experiments were performed at -80 mV in a solution comprising 1 M NaCl and 10 mM Tris•HCl (pH7.5). The concentrations of MC-RR, MC-LR and MC-YR were 200 μg/L each.

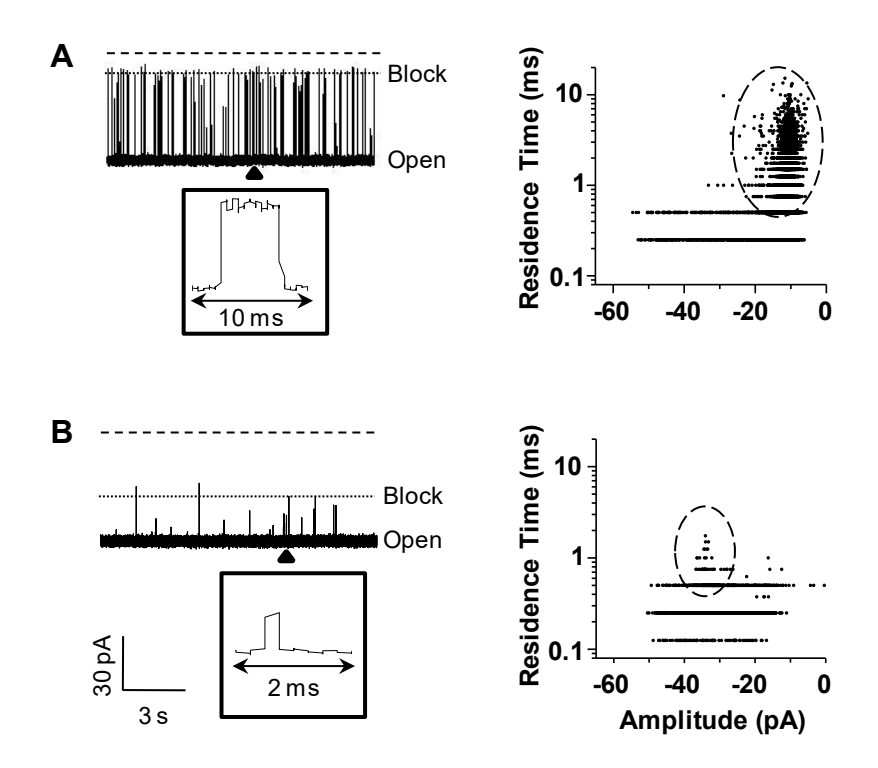


Figure 4. Differentiation of (A) cyclic MC-LR and (B) its linear analog via tryptic-digestion. (*Left*) Typical single-channel recording trace segments. Dashed lines represent the levels of zero current. Insets show enlarged images of arrow-marked events; and (*Right*) the corresponding scatter plots of event residence time vs. residual current. The experiments were performed at -80 mV with the wild-type α-hemolysin pore in a solution comprising 1 M NaCl and 10 mM Tris•HCl (pH7.5). The concentrations of MC-LR and its linear analog were 3.98 mg/L and 3.35 mg/L, respectively, while the concentration of trypsin was 150 ng/mL.

